Warm Dark Matter from theory and galaxy observations

H. J. de Vega

LPTHE, CNRS/Université P & M Curie (Paris VI).

Workshop CIAS Meudon 2012:

WARM DARK MATTER GALAXY FORMATION IN AGREEMENT WITH OBSERVATIONS

Observatoire de Paris, Château de Meudon, Meudon campus 6, 7 and 8 June 2012

tandard Cosmological Model: DM + Λ + Baryons + Radiati

- Begins by the inflationary era. Slow-Roll inflation explains horizon and flatness.
- Gravity is described by Einstein's General Relativity.
- Particle Physics described by the Standard Model of Particle Physics: $SU(3) \otimes SU(2) \otimes U(1) =$ qcd+electroweak model.
- Dark matter is non-relativistic during the matter dominated era where structure formation happens. DM is outside the SM of particle physics.
- Dark energy described by the cosmological constant Λ.

Standard Cosmological Model: ΛCDM $\Rightarrow$ ΛWDM

Dark Matter + Λ + Baryons + Radiation
begins by the Inflationary Era. Explains the Observations:

- Seven years WMAP data and further CMB data
- Light Elements Abundances
- Large Scale Structures (LSS) Observations. BAO.
- Acceleration of the Universe expansion:
  Supernova Luminosity/Distance and Radio Galaxies.
- Gravitational Lensing Observations
- Lyman α Forest Observations and X ray data
- Hubble Constant and Age of the Universe Measurements
- Properties of Clusters of Galaxies
- Galaxy structure explained by WDM

Dark Matter Particles

DM particles can decouple being ultrarelativistic (UR) or non-relativistic.
They can decouple at or out of thermal equilibrium.

The DM distribution function freezes out at decoupling.

The characteristic length scale is the free streaming scale (or Jeans' scale). For DM particles decoupling UR:

$$r_{lin} = 57.2\,\mathrm{kpc}\,\frac{\mathrm{keV}}{m}\,\left(\frac{100}{g_d}\right)^{\frac{1}{3}}$$

DM particles can freely propagate over distances of the order of the free streaming scale.

Therefore, structures at scales smaller or of the order r_{lin} are erased.

For $m \sim$ keV WDM particles $r_{lin} \sim 60$ kpc, is the size of the DM cores.

CDM free streaming scale

For CDM particles with $m \sim 100$ GeV: $r_{lin} \sim 0.1$ pc

Hence CDM structures keep forming till scales as small as the solar system.

This has been explicitly verified by all CDM simulations but never observed in the sky.

There is over abundance of small structures in CDM (also called the satellite problem).

Linear primordial power today $P(k)$ vs. k Mpc h

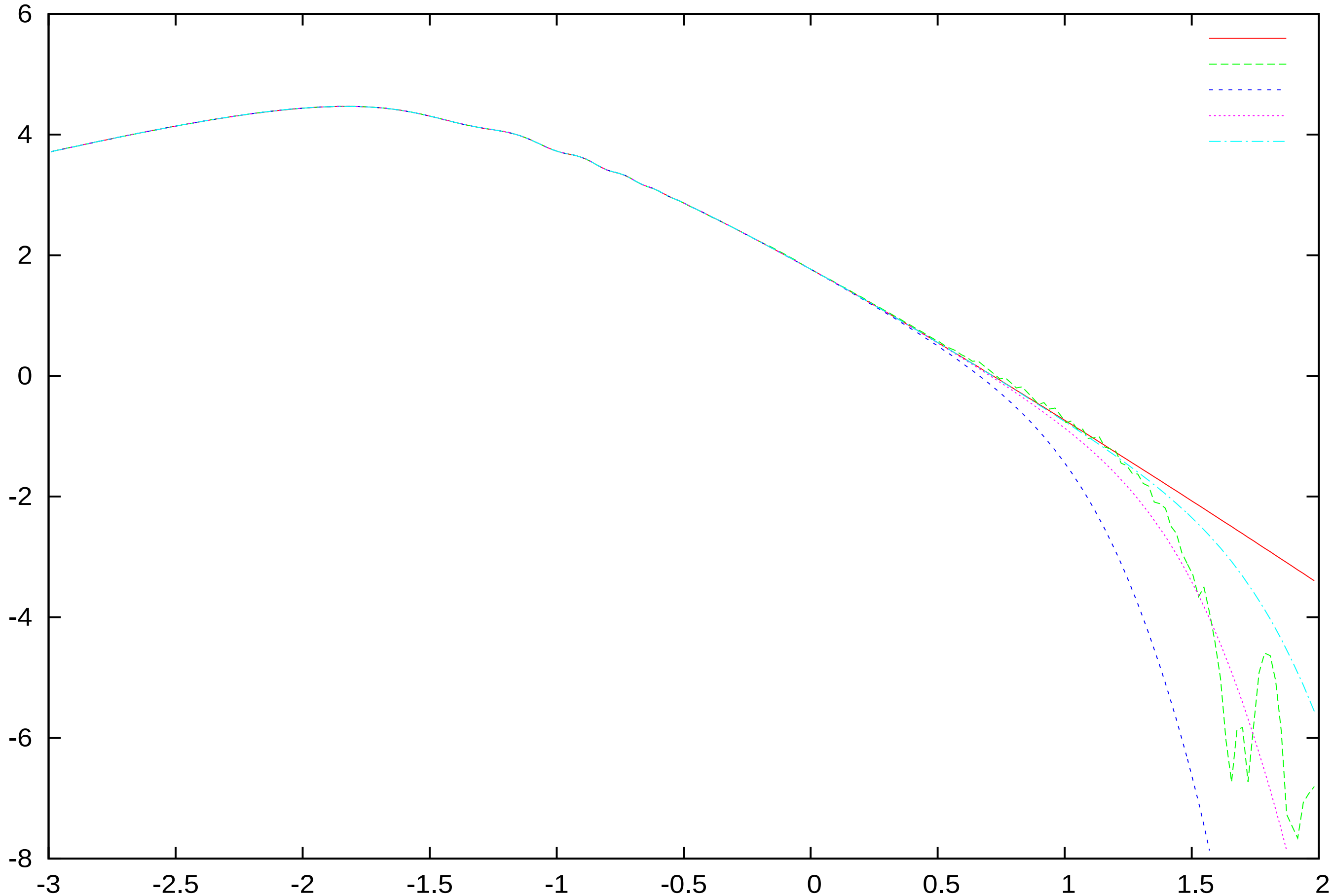

$\log_{10} P(k)$ vs. $\log_{10}[k \text{ Mpc } h]$ for CDM, 1 keV, 2 keV, light-blue 4 keV DM particles decoupling in equil, and 1 keV sterile neutrinos. WDM cuts $P(k)$ on small scales

$$r \lesssim 100\ (\text{keV}/m)^{4/3} \text{ kpc}$$

WDM vs. CDM linear fluctuations today

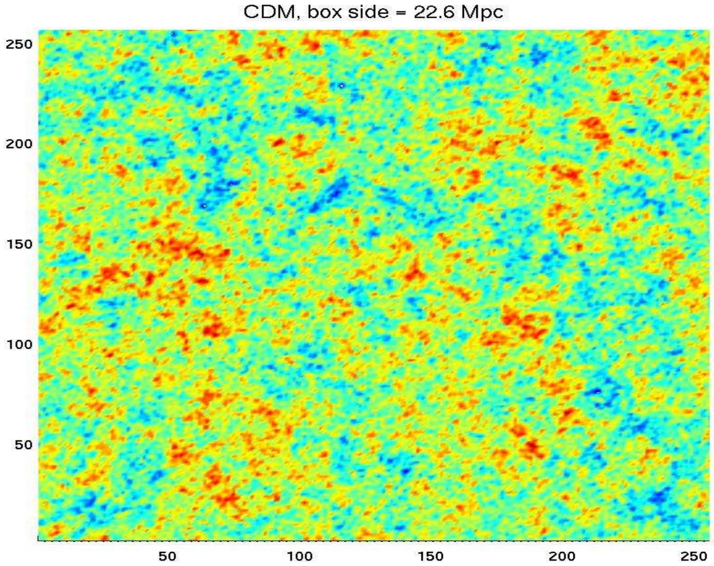

Box side = 22.6 Mpc. [C. Destri, private communication].

WDM:

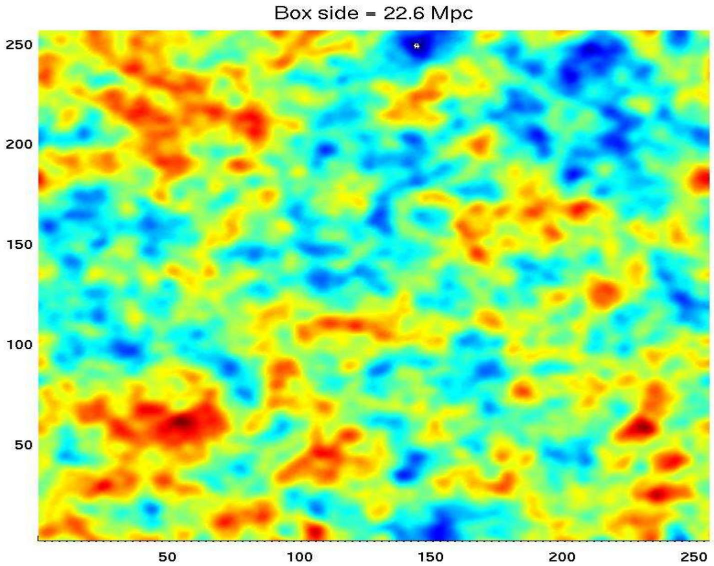

The expected overdensity

The expected overdensity within a radius R in the linear regime

$\sigma^2(R) = \int_0^\infty \frac{dk}{k}\, \Delta^2(k)\, W^2(kR) \quad , \quad W(kR)$: window function.

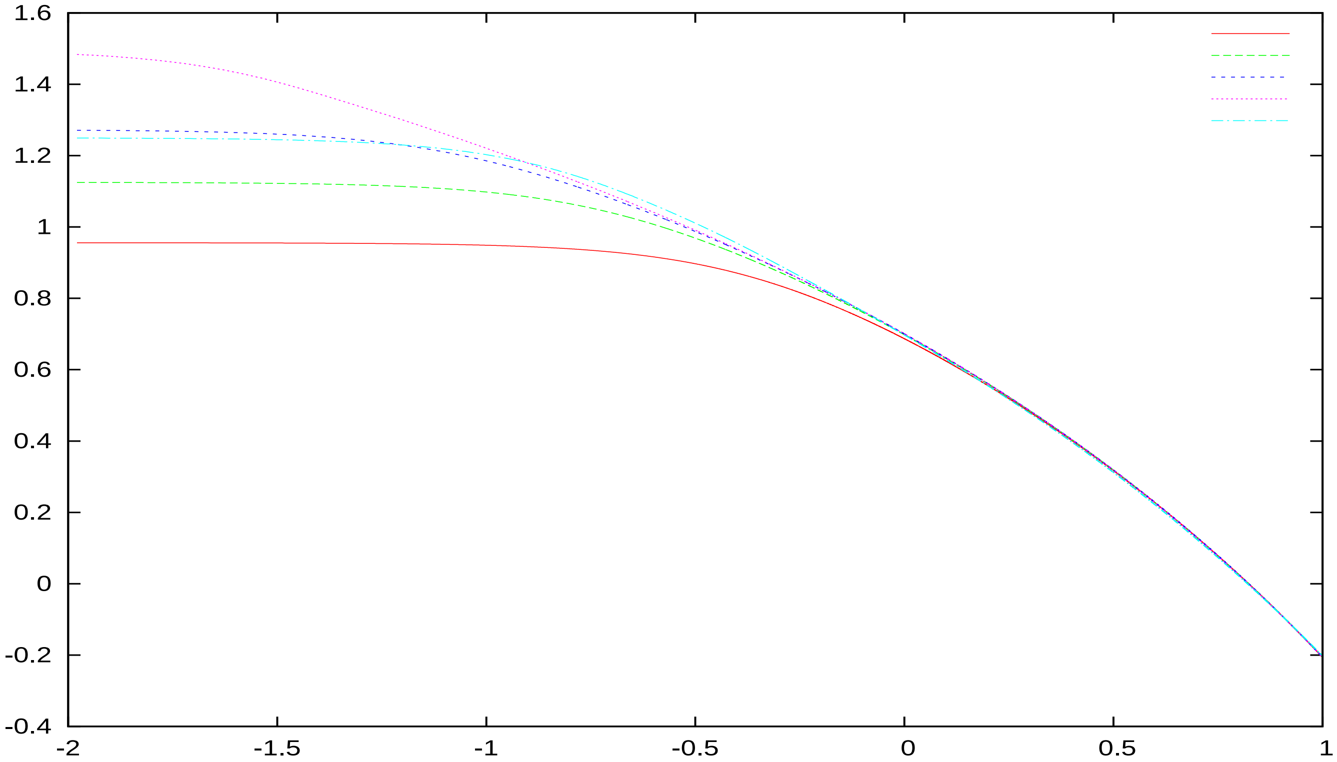

$\log \sigma(R)$ vs. $\log(R/h \text{ Mpc})$ for CDM, 1 keV, 2 keV, 4 keV DM particles decoupling in equil, and 1 keV (light-blue) sterile neutrinos. WDM flattens and reduces $\sigma(R)$ for small scales.

The Mass Function

The differential mass function gives the number of isolated bounded structures with mass between M and $M + dM$: (Press-Schechter)

$$\frac{dN}{dM} = -\frac{2\,\delta_c}{\sqrt{2\,\pi}\;\sigma^2(M,z)}\;\frac{\rho_M(z)}{M^2}\;\frac{d\sigma(M,z)}{d\ln M}\;e^{-\delta_c^2/[2\,\sigma^2(M,z)]},$$

$\delta_c = 1.686\ldots$: linear estimate for collapse from the spherical model.

$\sigma(M, z)$ is constant for WDM for small scales: small objects (galaxies) formation is suppresed in WDM in comparison with CDM.

$$\sigma(M, z) = \frac{g(z)}{z+1}\,\sigma(M, 0) \quad \text{during the MD/}\Lambda\text{ dominated era.}$$

$g(z)$: takes into account the effect of the cosmological constant, $g(0) = 0.76\ ,\ g(\infty) = 1$

$(M^2/\rho)\log dN/dM$ **vs.** $\log_{10} M/M_\odot$

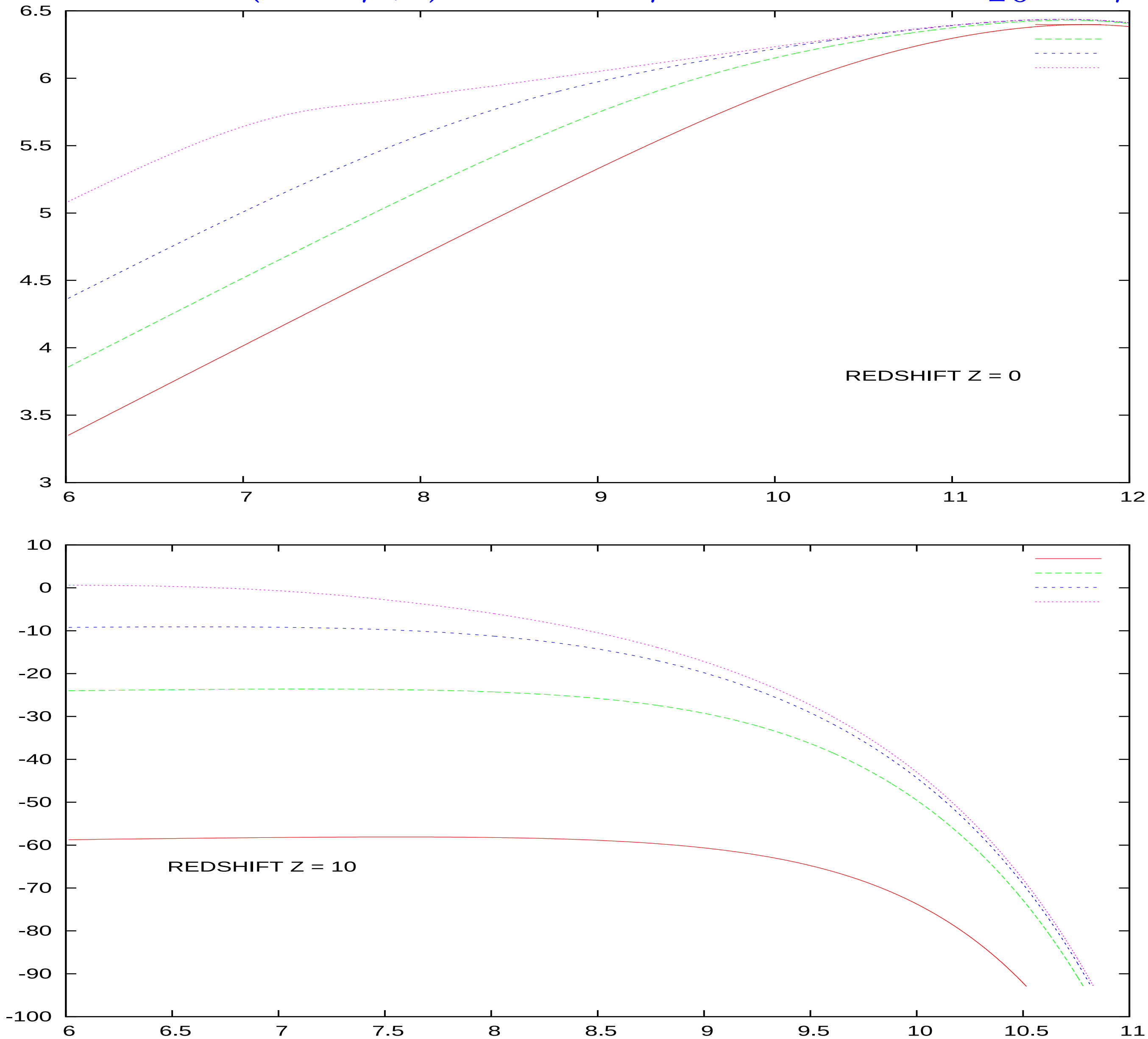

CDM, 1 keV, 2 keV, 4 keV WDM decoupling in equilibrium.

Galaxy Density Profiles: Cores vs. Cusps

Astronomical observations always find cored profiles for DM dominated galaxies. Selected references:
J. van Eymeren et al. A&A (2009), M. G. Walker, J. Peñarrubia, Ap J (2012). Reviews by de Blok (2010), Salucci & Frigerio Martins (2009).

Galaxy profiles in the linear regime: core size $\sim$ free streaming length (de Vega, Salucci, Sanchez, 2010)=

$$\text{halo radius } r_0 = \begin{cases} \sim 0.05 \text{ pc cusps for CDM (m} > \text{GeV).} \\ \sim 50 \text{ kpc cores for WDM (m} \sim \text{keV).} \end{cases}$$

N-body simulations for CDM give cusps (NFW profile).

N-body simulations for WDM : quantum physics needed for fermionic DM !!! (Destri, de Vega, Sanchez, 2012)

CDM simulations give a precise value for the concentration $\equiv R_{virial}/r_0$. CDM concentrations disagree with observed values.

The Phase-space density $Q(r)$

The phase-space density $Q \equiv \rho_{DM}/\sigma^3_{DM}$ is invariant under the cosmological expansion and can only decrease under self-gravity interactions (gravitational clustering).

Early universe value: $Q_{prim} = \rho_{prim}/\sigma^3_{prim} = \frac{3\sqrt{3}}{2\,\pi^2}\; g\; \frac{I_2^{\frac52}}{I_4^{\frac32}}\; m^4$

I_2 and I_4 are momenta of the DM distribution function.

g : $\#$ of internal degrees of freedom of the DM particle, $1 \leq g \leq 4$.

During structure formation Q decreases by a factor that we call $Z,\ (Z > 1)\ :\quad Q_{today} = \frac{1}{Z}\, Q_{prim}$

The Phase-space density $Q = \rho/\sigma^3$ and its decrease factor Z

The phase-space density today Q_{today} follows observing dwarf spheroidal satellite galaxies of the Milky Way (dSphs) as well as spiral galaxies. Its value is galaxy dependent.

For dSphs $Q_{today} \sim \ (0.18 \text{ keV})^4$ Gilmore et al. 07/08.

The spherical model gives $Z \simeq 41000$ and N-body simulations indicate: $10000 > Z > 1$. Z is galaxy dependent.

As a consequence m is in the keV scale:1keV$\lesssim m \lesssim 10$keV. H. J. de Vega, N. G. Sanchez, MNRAS (2010)

This is true both for DM decoupling in or out of equilibrium, bosons or fermions.

It is independent of the particle physics model.

ΛCDM and ΛWDM simulations vs. astronomical observations

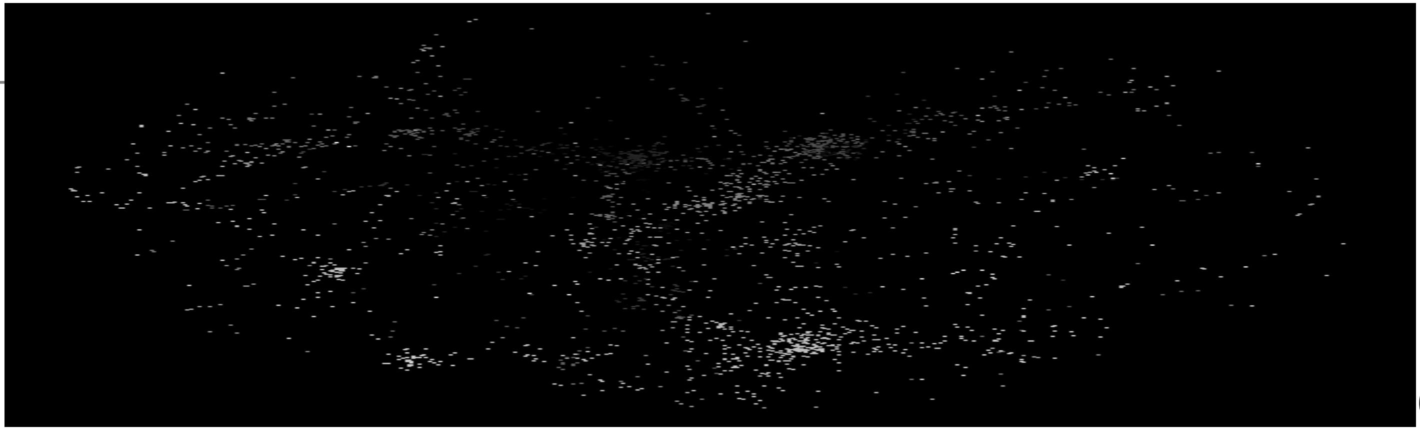

CDM

observations

1keV WDM

Quantum Bounds on Fermionic Dark Matter

The Pauli principle gives the upper bound to the phase space distribution function of spin-$\frac{1}{2}$ particles of mass m:

$$f(\vec{r},\vec{p}) \leq 2$$

The DM mass density is given by:

$$\rho(\vec{r}) = m \int d^3p \, \frac{f(\vec{r},\vec{p})}{(2\,\pi\,\hbar)^3} = \frac{m^4}{2\,\hbar^3}\, \sigma^3(\vec{r})\, \bar{f}(\vec{r})\, K \ ,$$

where:

$\bar{f}(\vec{r})$ is the $\vec{p}-$average of $f(\vec{r},\vec{p})$ over a volume $m^3\,\sigma^3(\vec{r})$,

$\sigma(\vec{r})$ is the DM velocity dispersion, $\sigma^2(\vec{r}) \equiv < v^2(\vec{r}) > /3$

$K \sim 1$ a pure number.

The Pauli bound $\bar{f}(\vec{r}) \leq 2$ yields: $Q(\vec{r}) \equiv \frac{\rho(\vec{r})}{\sigma^3(\vec{r})} \leq K\, \frac{m^4}{\hbar^3}$

This is an absolute quantum upper bound on $Q(\vec{r})$ due to quantum physics, namely the Pauli principle.

$Q(\vec{r})$ can **never** take values larger than $K\, m^4/\hbar^3$.

In the classical limit $\hbar \to 0$ and the bound disappears.

Classical physics breaks down near the galaxy center

N-body simulations point to cuspy phase-space densities

$Q(r) = Q_s \left(\frac{r}{r_s}\right)^{-\beta}, \quad \beta \simeq 1.9 - 2, \;\; r_s =$ halo radius,

$Q_s =$ mean phase space density in the halo.

$Q(r)$ derived within classical physics tends to infinity for $r \to 0$ violating the Pauli principle bound.

Classical physics breaks down near the galaxy center.

For $\beta = 2$ the quantum upper bound on $Q(r)$ is valid for

$$r \geq r_q \equiv \frac{\hbar^{\frac{3}{2}}}{m^2} \sqrt{\frac{Q_s}{K}}\, r_s \; .$$

Observations yield: $30 < \frac{r_s}{\mathrm{pc}} < 5.10^4 \; , \; 2.10^{-5} < \frac{\hbar^{\frac{3}{2}} \sqrt{Q_s}}{(\mathrm{keV})^2} < 0.6$

The larger Q_s and the smaller r_s correspond to ultra compact dwarfs

The smaller Q_s and the larger r_s correspond to spirals.

Quantum bounds on the galaxy core size

Combining the virial theorem

$$\sigma_s^2 = \frac{G\,M_s}{3\,r_s} \quad \text{and} \quad M_s = \frac{4}{3}\,\pi\,r_s^3\,\rho_s$$

with the quantum bound on $Q(r)$ yields that classical physics breaks down for $r < r_q$ where

$$r_q = \frac{1.5 \times 3^{\frac{1}{4}}}{\sqrt{\pi\;K}\;m^2} \left(\frac{\hbar}{\sqrt{G}}\right)^{\frac{3}{2}} \left(\frac{r_s}{M_s}\right)^{\frac{1}{4}} = \frac{0.5879}{\sqrt{K}} \left(\frac{r_s}{\mathrm{pc}}\;\frac{10^6\,M_\odot}{M_s}\right)^{\frac{1}{4}} \left(\frac{\mathrm{keV}}{m}\right)^2 \;\mathrm{pc}$$

Conclusion: r_q is in the parsec range for WDM $m \sim$ keV.

r_q is the minimal possible value for the core radius.

The core radius can be well above r_q which corresponds to maximally packed fermions around the center of the galaxy.

For diluted objects as galaxies core radii much larger than r_q are expected.
In atoms the electrons phase-space density turns to be significantly below the Pauli quantum bound.

The quantum radius r_q for different kinds of DM

DM type	DM particle mass	r_q	
CDM	$1 - 100$ GeV	$1 - 10^4$ meters	in practice zero
WDM	$1 - 10$ keV	$0.1 - 1$ pc	compatible with observed cores
HDM	$1 - 10$ eV	kpc - Mpc	too big !

Dwarf galaxies as quantum objects

de Broglie wavelength of DM particles $\lambda_{dB} = \frac{1}{m \, \sigma}$

$d =$ Average distance between particles

$d = \left(\frac{m}{\rho}\right)^{\frac{1}{3}} \quad , \quad \rho = \sigma^3 \, Q \quad , \quad Q =$ phase space density.

ratio: $\mathcal{R} = \frac{\lambda_{dB}}{d} = \left(\frac{Q}{m^4}\right)^{\frac{1}{3}}$

Observed values: $0.74 \times 10^{-3} < \mathcal{R} \left(\frac{m}{\mathrm{keV}}\right)^{\frac{1}{3}} < 0.70$

The larger $\mathcal{R}$ is for ultracompact dwarfs.
The smaller $\mathcal{R}$ is for big spirals.

The ratio $\mathcal{R}$ near unity (or above) means a QUANTUM OBJECT.

Observations alone show that compact dwarf galaxies are quantum objects (for WDM).

Summary on quantum bounds on cores

- If DM were formed by bosons the quantum bound on Q does not apply and the formation of cusps would be allowed.
- Astronomical observations show that DM galaxy density profiles are cored.
- Thus, bosonic DM turns to be strongly disfavoured.
- In all cases, cusps of fermionic DM in the galaxy density profile are artifacts produced by classical physics computations irrespective of the nature of dark matter (HDM, WDM, CDM).
- Quantum physics, namely the Pauli principle, rule out galaxy cusps for fermionic dark matter.
- C. Destri, H. J. de Vega, N. G. Sanchez, 'Fermionic warm dark matter produces galaxy cores in the observed scales', arXiv:1204.3090.

WDM properties

WDM is characterized by

- its initial power spectrum cutted off for scales below ~ 50 kpc. Thus, structures are not formed in WDM for scales below ~ 50 kpc.
- its initial velocity dispersion. However, this is negligible for $z < 100$ where the non-linear regime starts.
- Classical N-body simulations break down at small distances ($\sim$ pc). Need of quantum calculations to find WDM cores.

Structure formation is hierarchical in CDM.

WDM simulations show in addition top-hat structure formation at large scales and low densities but hierarchical structure formation remains dominant.

Quantum pressure vs. gravitational pressure

quantum pressure: $P_q =$ flux of momentum $= n\ v\ p$,
$v =$ mean velocity, momentum $= p \sim \hbar/\Delta x \sim \hbar\ n^{\frac{1}{3}}$,
particle number density $= n = \frac{M_q}{\frac{4}{3}\ \pi\ R_q^3\ m}$

galaxy mass $= M_q$, galaxy halo radius $= R_q$

gravitational pressure: $P_G = \frac{G\ M_q^2}{R_q^2} \times \frac{1}{4\ \pi\ R_q^2}$

Equilibrium: $P_q = P_G \Longrightarrow M_q = \frac{9}{2\ \sqrt{\pi}\ m^2}\ \left(\frac{\hbar\ v}{G}\right)^{\frac{3}{2}} =$

$$= 0.797\ldots 10^6\ M_\odot\ \left(\frac{\mathrm{keV}}{m}\right)^2 \left(\frac{v}{10\ \frac{\mathrm{km}}{\mathrm{s}}}\right)^{\frac{3}{2}}$$

for WDM $M_q \sim$ mass of dwarf galaxies !!

Dwarf spheroidal galaxies can be supported by the fermionic quantum pressure of WDM.

Self-gravitating Fermions in the Thomas-Fermi approach

WDM is non-relativistic in the MD era.

Chemical potential: $\mu(r) = \mu_0 - m\,\phi(r)$,

$\phi(r) =$ gravitational potential.

Poisson's equation: $\frac{d^2\mu}{dr^2} + \frac{2}{r}\,\frac{d\mu}{dr} = -4\,\pi\,G\,m\,\rho(r)$

$\rho(0) =$ finite for fermions $\Longrightarrow \frac{d\mu}{dr}(0) = 0$.

Density $\rho(r)$ in terms of the distribution function $f(E)$:

$$\rho(r) = \frac{m}{\pi^2\,\hbar^3}\int_0^\infty p^2\,dp\;f[\frac{p^2}{2\,m} - \mu(r)]$$

Thomas-Fermi approximation: system of ordinary nonlinear differential equations. Determine the chemical potential $\mu(r)$

Boundary condition: $r = R = R_{200} \sim R_{vir}$.

At $r = R_{200}$ the DM density $\simeq 200\;\bar{\rho}_{DM}$.

Self-gravitating Fermions 2

In dimensionless variables the Thomas-Fermi equations for self-gravitating fermions:

$$\frac{d^2\nu}{d\xi^2} + \frac{2}{\xi}\,\frac{d\nu}{d\xi} + 3\,\beta(\nu(\xi)) = 0 \quad , \quad \beta(\nu) \equiv \int_0^\infty y^2\,dy\,\Psi(y^2-\nu)$$

Here: $\mu(r) = E_0\,\nu(\xi) \quad , \quad r = L_0\,\xi \quad , \quad f(E) = \Psi\left[\frac{E}{E_0}\right]$

$E_0 =$ characteristic energy of DM particles at decoupling.

$L_0 =$ characteristic length.

L_0 emerges from the fermion dynamics in Thomas-Fermi

$$L_0 \equiv \frac{\sqrt{3\,\pi\,\hbar^3}}{\sqrt{G}\,(2\,m)^2}\,\left(\frac{2\,m}{E_0}\right)^{\frac{1}{4}} \quad , \quad \rho(r) = \frac{m^4}{\pi^2\,\hbar^3}\,\left(\frac{2\,E_0}{m}\right)^{\frac{3}{2}}\,\beta(\nu(\xi))$$

Thermal equilibrium: $\Psi_{FD}(x) = \dfrac{1}{e^x+1}\,,$

Dodelson-Widrow: $\Psi_{DW}(x) = \dfrac{f_0}{m}\,\dfrac{1}{e^x+1}\,,\ f_0 \simeq 0.043$ keV

ν-MSM model: $\Psi_{\nu-MSM}(x) = 2\,\tau\,\sqrt{\frac{\pi}{x}}\sum_{n=1}^\infty \dfrac{e^{-n\,x}}{n^{\frac{5}{2}}}\,,\ \tau \simeq 0.03$

Thomas-Fermi approximation: solutions

$$M(R) = \frac{(3\,\pi)^2\,\hbar^6}{256\,G^3\,m^8\,R^3}\;\;\xi_0^5\;\;|\nu'(\xi_0)| = \text{total mass.}$$

$$P(r) = \frac{\pi^{\frac{4}{3}}}{3}\;\hbar^2\;\left[\frac{\rho(0)}{\beta(\xi_0)\;m^4}\right]^{\frac{5}{3}}\;\int_0^\infty y^4\,dy\;\Psi\left(y^2 - \nu(\xi)\right)$$

L_0 and $M(R)$ turn to be of the order of the Jeans' length and the Jeans' mass, respectively.

The chemical potential at $r = 0$ fixed by the value of $Q(0)$.

Using observed values of $Q(0)$, we obtain halo radius $r_s \sim 0.1 - 10$ kpc, galaxy masses $10^5 - 10^7\;M_\odot$ and velocity dispersions, all consistent with the observations of dwarf galaxies.

The Thomas-Fermi approach gives realistic halo radii, larger than the quantum lower bound r_q, as expected.

Fermionic WDM treated quantum mechanically is able to reproduce the observed DM cores of galaxies.

Sterile Neutrinos in the SM of particle physics

SM symmetry group: $SU(3)_{color} \otimes SU(2)_{weak} \otimes U(1)^{weak}_{hypercharge}$

Leptons are color singlets and doublets under weak SU(2).

Sterile neutrinos ν_R do not participate to weak interactions. Hence, they must be singlets of color, weak SU(2) and weak hypercharge.

The SM Higgs Φ is a SU(2) doublet with a nonzero vacuum expectation value Φ_0. It can couple Yukawa-type with the left and right handed leptons:

$$L_{Yuk} = y \, \bar{\nu}_L \, \nu_R \, \Phi_0 + h.c. \quad ,$$

$y =$ Yukawa coupling, $\Phi_0 = \begin{pmatrix} 0 \\ v \end{pmatrix} \quad , \quad v = 174$ GeV.

This induces a mixing (bilinear) term between ν_L and ν_R which produces transmutations of $\nu_L \Leftrightarrow \nu_R$.

Sterile Neutrinos Mixing

Mixing and oscillations of particle states are typical of low energy particle physics !

- Flavor mixing: e-μ neutrino oscillations (explain solar neutrinos).
- $K^0 - \overline{K}^0, B^0 - \overline{B}^0$ and $D^0 - \overline{D}^0$ meson oscillations in connection with CP-violation.

Neutrino mass matrix: $(\bar{\nu}_L \ \bar{\nu}_R) \begin{pmatrix} 0 & m_D \\ m_D & M \end{pmatrix} \begin{pmatrix} \nu_L \\ \nu_R \end{pmatrix}$

$M =$ right-neutrino mass, $m_D = y \ v \ , \ M \gg m_D$. Seesaw.

Mass eigenvalues: $\frac{m_D^2}{M}$ and M, with eigenvectors:

- active neutrino: $\nu_{active} \simeq \nu_L - \frac{m_D}{M} \ \nu_R$.
- sterile neutrino: $\nu_{sterile} \simeq \nu_R + \frac{m_D}{M} \ \nu_L, \quad M \gg m_D^2/M$.

Sterile Neutrinos

Choosing $M \sim 1$ keV and $m_D \sim 0.1$ eV is consistent with observations.

Mixing angle: $\theta \sim \frac{m_D}{M} \sim 10^{-4}$ is appropriate to produce enough sterile neutrinos accounting for the observed DM.

Smallness of θ makes sterile neutrinos difficult to detect.

Precise measure of nucleus recoil in tritium beta decay: ${}^3H_1 \Longrightarrow {}^3He_2 + e^- + \bar{\nu}$ can show the presence of a sterile instead of the active $\bar{\nu}$ in the decay products.

Rhenium 187 beta decay gives $\theta < 0.095$ for 1 keV steriles [Galeazzi et al. PRL, 86, 1978 (2001)].
Available energy: $Q({}^{187}Re) = 2.47$ keV, $Q({}^3H_1) = 18.6$ keV.

Conclusion: the empty slot of right-handed neutrinos in the Standard Model of particle physics can be filled by keV-scale sterile neutrinos describing the DM.

Sterile neutrino models

Sterile neutrinos: named by Bruno Pontecorvo (1968).

- DW: Dodelson-Widrow model (1994) sterile neutrinos produced by non-resonant mixing from active neutrinos.
- Shi-Fuller model (1998) sterile neutrinos produced by resonant mixing from active neutrinos.
- ν-MSM model (1981)-(2006) sterile neutrinos produced by a Yukawa coupling from a real scalar χ.
- DM models must reproduce $\bar{\rho}_{DM}$, galaxy and structure formation and be consistent with particle experiments.

WDM particles in different models behave just as if their masses were different:

$$\frac{m_{DW}}{\text{keV}} \simeq 4.4 \left(\frac{m_{Thermal}}{\text{keV}}\right)^{4/3}, \; m_{DW} \simeq 1.5 \, m_{SF}, \; m_{SF} \simeq 3 \, m_{\nu\text{MSM}}.$$

H J de Vega, N Sanchez, Phys. Rev. D85, 043517 (2012).

Further Experiments to detect Sterile Neutrinos

Lyα forest observations give limits on the sterile ν mass. However, it is the most sensitive method to the difficult-to-characterize non-linear growth of baryonic and DM structures. As a result, there are significant discrepancies between the reported mass lower limits.

Supernovae: θ unconstrained, $1 < m < 10$ keV (G. Raffelt & S. Zhou, PRD 2011).

CMB: WDM decay distorts the blackbody CMB spectrum. The projected PIXIE satellite mission (A. Kogut et al.) can measure WDM sterile neutrino mass.

Rhenium and Tritium beta decay (MARE, KATRIN). Theoretical analysis: H J de V, O. Moreno, E. Moya de Guerra, M. Ramón Medrano, N. Sánchez, arXiv:1109.3452.

Sterile Neutrinos may be observed in electron capture (EC) as in ^{163}Ho $\rightarrow$ ^{163}Dy, MARE experiment (Nuccioti et al.)

Summary: keV scale DM particles

- Reproduce the phase-space density observed in dwarf spheroidal and spiral galaxies (dV S, MNRAS 2010).
- Fermionic WDM provide cored galaxy profiles through quantum effects in agreement with observations (Destri, de Vega, Sanchez, 2012).
- The galaxy surface density $\mu_0 \equiv \rho_0 \, r_0$ is universal up to $\pm 10\%$ according to the observations. Its value $\mu_0 \simeq (18 \text{ MeV})^3$ is reproduced by WDM (dV S S, New Astronomy, 2012). CDM simulations give 1000 times the observed value of μ_0 (Hoffman et al. ApJ 2007).
- Alleviate the satellite problem which appears when wimps are used (Avila-Reese et al. 2000, Götz & Sommer-Larsen 2002, Markovic et al. JCAP 2011)
- Alleviate the voids problem which appears when wimps are used (Tikhonov et al. MNRAS 2009).

Summary: keV scale DM particles

- All direct searches of DM particles look for $m \gtrsim 1$ GeV. DM mass in the keV scale explains why nothing has been found ... e^+ and $\bar{p}$ excess in cosmic rays may be explained by astrophysics: P. L. Biermann et al. PRL (2009), P. Blasi, P. D. Serpico PRL (2009).
- Velocity widths in galaxies from 21cm HI surveys. ALFALFA survey clearly favours WDM over CDM. Papastergis et al. ApJ 2011, Zavala et al. ApJ 2009
- Combining theoretical evolution of fluctuations through the Boltzmann-Vlasov equation with galaxy data points to a DM particle mass 3 - 10 keV. The keV mass scale holds independently of the DM particle physics model.
- Highlights and conclusions of the Chalonge Meudon Workshop 2011: Warm dark matter in the galaxies, arXiv:1109.3187 and the 16th Paris Cosmology Colloquium 2011 arXiv:1203.3562, H. J. de V., N. G. S.

Summary and Conclusions

- Combining theoretical evolution of fluctuations through the Boltzmann-Vlasov equation with galaxy data points to a DM particle mass 3 - 10 keV. T_d turns to be model dependent. The keV mass scale holds independently of the DM particle physics model.
- Universal Surface density in DM galaxies [$\mu_{0D} \simeq (18 \text{ MeV})^3$] explained by keV mass scale DM. Density profile scales and decreases for intermediate scales with the spectral index n_s : $\rho(r) \sim r^{-1-n_s/2}$ and $\rho(r) \sim r^{-2}$ for $r \gg r_0$.

H. J. de Vega, P. Salucci, N. G. Sanchez, 'The mass of the dark matter particle from theory and observations', New Astronomy, 17, 653 (2012).

H. J. de Vega, N. Sanchez, 'Model independent analysis of dark matter points to a particle mass at the keV scale', MNRAS 404, 885 (2010).

Future Perspectives

DM properties from galaxy observations.

Chandra, Suzaku X-ray data: keV mass DM decay?

Sun models well reproduce the sun's chemical composition but not the heliosismology (Asplund et al. 2009).
Can DM inside the Sun help to explain the discrepancy?

Nature of Dark Matter? 83% of the matter in the universe.
Light DM particles are strongly favoured $m_{DM} \sim$ keV.
Sterile neutrinos ? Other particle in the keV mass scale?

Precision determination of DM properties (mass, T_d, nature) from better galaxy data combined with theory (Boltzmann-Vlasov and simulations).

Extensive WDM N-body simulations showing substructures, galaxy formation and evolution.
Quantum dynamical evolution to compute WDM cores.

Bounds from MARE on sterile neutrino mass and θ.
Could KATRIN join the search of sterile neutrinos?

The Universe is our ultimate physics laboratory

THANK YOU VERY MUCH

FOR YOUR ATTENTION!!

The Free Streaming Scale

The characteristic length scale is the free streaming scale (or Jeans' scale)

$$r_{lin} = 2\,\sqrt{1+z_{eq}}\,\left(\frac{3\,M_{Pl}^2}{H_0\,\sqrt{\Omega_{DM}}\;Q_{prim}}\right)^{\frac{1}{3}} = 21.1\,q_p^{-\frac{1}{3}}\text{ kpc}$$

$q_p \equiv Q_{prim}/(\mathrm{keV})^4$. DM particles can freely propagate over distances of the order of the free streaming scale.

$$r_{lin} = 57.2\,\mathrm{kpc}\,\frac{\mathrm{keV}}{m}\,\left(\frac{100}{g_d}\right)^{\frac{1}{3}}$$

Therefore, structures at scales smaller or of the order r_{lin} are erased.

It is useful to introduce the dimensionless wavenumber:

$$\gamma \equiv k\,r_{lin}/\sqrt{3} \quad \text{and} \quad \alpha \equiv \sqrt{3}\,\gamma/\sqrt{I_4}$$

where I_4 is the second momentum of the DM zeroth order distribution.

Relics decoupling non-relativistic

$$F_d^{NR}(p_c) = \frac{2^{\frac{5}{2}}\,\pi^{\frac{7}{2}}}{45}\;g_d\,Y_\infty\;\left(\frac{T_d}{m}\right)^{\frac{3}{2}}\;e^{-\frac{p_c^2}{2\,m\,T_d}} = \frac{2^{\frac{5}{2}}\,\pi^{\frac{7}{2}}}{45}\;\frac{g_d\,Y_\infty}{x^{\frac{3}{2}}}\;e^{-\frac{y^2}{2\,x}}$$

$Y(t) = n(t)/s(t),\; n(t)$ number of DM particles per unit volume, $s(t)$ entropy per unit volume, $x \equiv m/T_d,\; T_d < m$.

$Y_\infty = \frac{1}{\pi}\,\sqrt{\frac{45}{8}}\;\frac{1}{\sqrt{g_d}\;T_d\;\sigma_0\;M_{Pl}}$ late time limit of Boltzmann.

σ_0: thermally averaged total annihilation cross-section times the velocity.

From our previous general equations for m and g_d:

$m = \frac{45}{4\,\pi^2}\;\frac{\Omega_{DM}\;\rho_c}{g\;T_\gamma^3\;Y_\infty} = \frac{0.748}{g\;Y_\infty}$ eV and $m^{\frac{5}{2}}\;T_d^{\frac{3}{2}} = \frac{45}{2\,\pi^2}\;\frac{1}{g\;g_d\;Y_\infty}\;Z\;\frac{\rho_s}{\sigma_s^3}$

Finally: $\sqrt{m\;T_d} = 1.47\;\left(\frac{Z}{g_d}\right)^{\frac{1}{3}}\,\mathrm{keV}$

We used ρ_{DM} today and the decrease of the phase space density by a factor Z.

Relics decoupling non-relativistic 2

Allowed ranges for m and T_d.

$m > T_d > b$ eV where $b > 1$ or $b \gg 1$ for DM decoupling in the RD era

$$\left(\frac{Z}{g_d}\right)^{\frac{1}{3}} \; 1.47 \text{ keV} < m < \frac{2.16}{b} \text{ MeV} \; \left(\frac{Z}{g_d}\right)^{\frac{2}{3}}$$

$g_d \simeq 3 \quad \text{for} \quad 1 \text{ eV} < T_d < 100 \text{ keV}$ and $1 < Z < 10^3$

$1.02 \text{ keV} < m < \frac{104}{b} \text{ MeV} \quad , \quad T_d < 10.2$ keV.

Only using ρ_{DM} today (ignoring the phase space density information) gives one equation with three unknowns: $m, \; T_d$ and σ_0,

$\sigma_0 = 0.16 \text{ pbarn} \, \frac{g}{\sqrt{g_d}} \, \frac{m}{T_d}$ http://pdg.lbl.gov

WIMPS with $m = 100$ GeV and $T_d = 5$ GeV require $Z \sim 10^{23}$.

Universe Inventory

The universe is spatially flat: $ds^2 = dt^2 - a^2(t)\, d\vec{x}^2$ plus small primordial fluctuations.

Dark Energy (Λ): 74 % $\quad , \quad$ Dark Matter: 21 %

Baryons $+$ electrons: 4.4 % $\;,\;$ Radiation ($\gamma + \nu$): 0.0085%

83 % of the matter in the Universe is DARK.

$$\rho(\text{today}) = 0.974\ 10^{-29}\ \frac{\text{g}}{\text{cm}^3} = 5.46\ \frac{\text{GeV}}{\text{m}^3} = (2.36\ 10^{-3}\ \text{eV})^4$$

DM dominates in the halos of galaxies (external part).

Baryons dominate around the center of galaxies.

Galaxies form out of matter collapse. Since angular momentum is conserved, when matter collapses its velocity increases. If matter can loose energy radiating, it can fall deeper than if it cannot radiate.

Velocity widths in galaxies

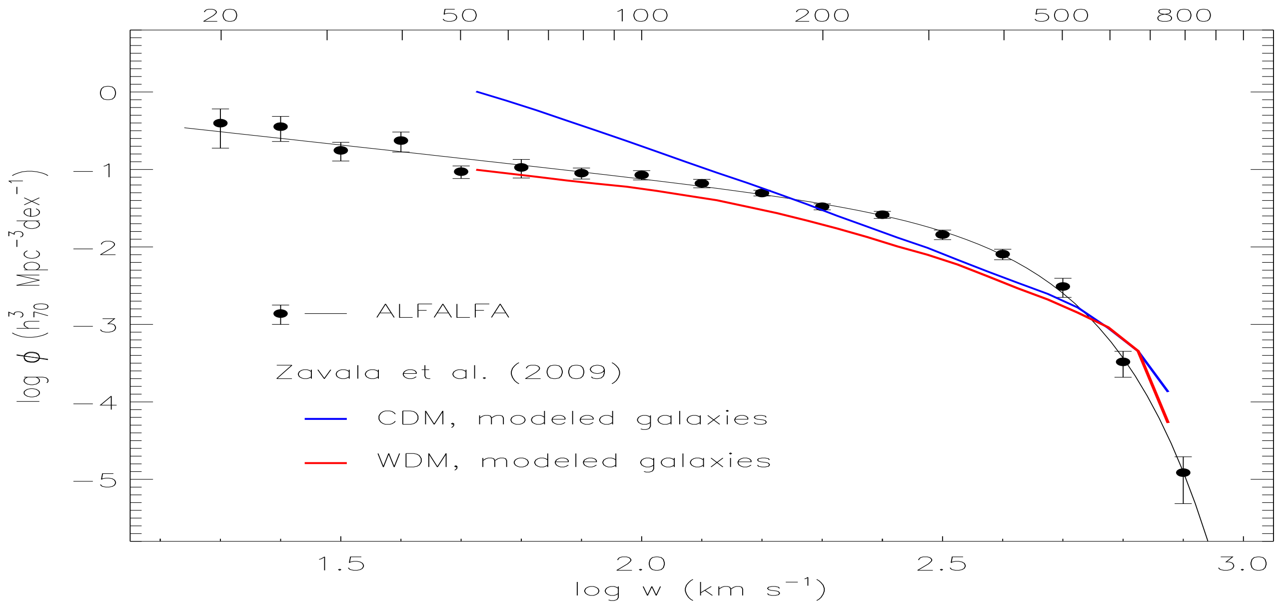

Velocity widths in galaxies from 21cm HI surveys. ALFALFA survey clearly favours WDM over CDM. (Papastergis et al. 2011, Zavala et al. 2009).

Notice that the WDM red curve is for $m = 1$ keV WDM particle decoupling at thermal equilibrium.

The 1 keV WDM curve falls somehow below the data suggesting a slightly larger WDM particle mass.